ILASS–Europe 2022, 31th Conference on Liquid Atomization and Spray Systems, 6-8 September 2022, Virtual, Israel

Preferential accumulation of evaporating poly-disperse droplets in zero-mean homogeneous and isotropic turbulence

Nandhakumar Pandurangan* and Srikrishna Sahu
Department of Mechanical Engineering, Indian Institute of Technology Madras, Chennai – 600 036, India
*Corresponding author: nandhakumariitm08@gmail.com

Abstract
In this work, we consider the interaction of evaporating polydispersed droplets with homogenous and isotropic turbulence (HIT) without mean flow in an open chamber, which is achieved by using several synthetic jet actuators. A twin-fluid atomizer is employed to inject acetone droplets from the top of the box. The experiments are repeated with water droplets as well. The clusters are characterized by the application of Voronoi analysis on particle image velocimetry images of the droplets. The droplet size is measured using Interferometric Laser Imaging for Droplet Sizing (ILIDS) technique. The PDF of the cluster area remains almost unaltered for acetone droplets with HIT. But the PDF shifts to the right for water droplets, indicating the formation of many large clusters. Acetone droplets form more small-scale clusters than water droplets for similar turbulent intensity, but the degree of droplet clustering is almost the same for both in the presence of HIT.

Keywords
Isotropic turbulence, box of turbulence, Preferential concentration, Droplet clustering, Voronoi analysis.

1. Introduction

Spray dispersion and evaporation are prevalent phenomena that occur during many industrial processes and applications, such as spray drying, spray painting, and liquid fuel spray combustion, for instance, in IC engines and gas turbines. Sprays always tend to entrain the surrounding air, which is turbulent, and in such a case, the droplets have a tendency to distribute inhomogeneously in space, forming clusters and depleted regions. This phenomenon is referred as “preferential concentration” effect [1]. The tendency of particles able to preferentially accumulate and form clusters is assessed by a non-dimensional number called Stokes number (*St*). If $St << 1$, the droplet follows the flow like a tracer particle. When $St >> 1$, the droplet does not respond to the flow. On the other hand, when $St \approx 1$, the droplet partially responds to the flow and forms clusters.

For a spray, droplet clustering can be crucial since the instantaneous spatial distribution of droplets in sprays might have dense and dilute regions, which strongly influence the subsequent evaporation of droplets and the process of air-fuel mixture preparation. The Stokes number is proportional to the square of the droplet diameter. The evaporation causes a reduction in droplet diameter, so *St* changes for an evaporating droplet. Due to variation in *St* during its transport, the response of an evaporating droplet to surrounding turbulence may change significantly. Turbulence, droplet dispersion, and droplet evaporation are interlinked for liquid sprays. Hence, it is essential to investigate the interaction among those.

Considering that particle-turbulence interaction is a complex physical phenomenon, understanding the droplet behavior homogenous and isotropic turbulence (HIT) is an important step to gain fundamental insight into the problem and also to develop models. In the past, researchers have proposed different methods to produce homogenous and isotropic turbulence. The primary approach has been to use a grid in the wind tunnel, which generates nearly isotropic turbulence. Some limitations in this approach are that turbulence is always associated with the finite mean flow, a long development length from the grid is needed for

the turbulence to become approximately isotropic, and the turbulence intensities generated by grids decay in space and are typically low [2]. To overcome the above mentioned difficulties, a box-of-turbulence is used where isotropic turbulence is created within an open/closed chamber using fans or synthetic jets. Birouk et al. [3] produced HIT with zero mean flow by using eight electrical fans at the corners of a cubic chamber. Hwang and Eaton [2] used synthetic jet actuators instead of fans at the corners of a cube to produce HIT with a small mean flow and studied the clustering of monodispersed solid particles. Charalampous and Hardalupas [4] developed a setup similar to Hwang and Eaton. Goepfert et al. [5] and Ujas & Sahu [6] built a similar kind of box-type turbulence chamber, but they modified the setup by changing the positions of jet actuators. They kept the jet actuators at the faces of a cube, so they utilized only six actuators to produce nearly zero mean, homogenous and isotropic turbulence. A few works focused on droplet clustering in zero mean, homogenous and isotropic turbulence that too without considering evaporating nature of droplets. In this work, the primary aim is to study the clustering of evaporating acetone droplets in such a turbulent environment.

2. Material and Methods

2.1. Experimental setup

In this work, stationary homogenous and isotropic turbulence (HIT) with zero mean is achieved using synthetic jet actuators. The experimental rig is shown in Fig 1. The details of the experimental setup are given in Patel and Sahu [6]; here, a brief explanation is provided. Six synthetic jet actuators (Ahuja: AS12X100 PA; dimension of each speaker is 300 mm; the rms of power rating is 100 W) are arranged on aluminium rails in such a way that they face a common center. Plates with holes are used to cover the front side of the speaker to produce high-velocity jets. The holes are placed as a two-dimensional array of a hexagonal pattern (80 holes of 6 mm diameter). The actuators are connected to amplifiers which are controlled by a 16-bit National Instrument card (NI: PCI 6733). A digital sinusoidal signal with a fixed frequency (50 Hz) is generated by an in-house lab view code and continuously fed into the NI card. It converts the digital signal to an analog signal and supplied it to the amplifiers. Each amplifier is connected to two speakers placed opposite each other. The amplitude of each speaker is individually controlled, and by varying the speaker's amplitude, different turbulence intensity is obtained. Due to associated noise with the speakers and the electrical equipment, some fine-tuning of amplitude is always necessary to achieve the HIT.

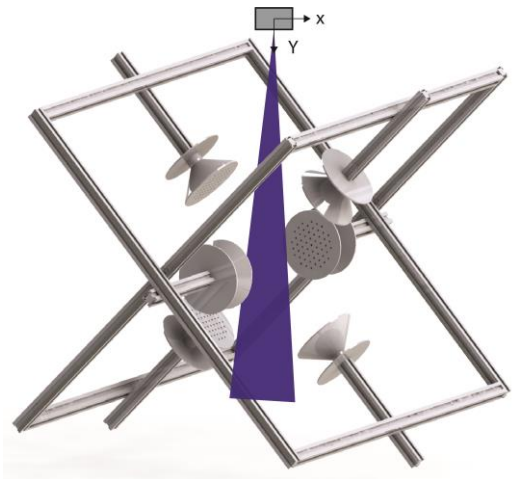

Figure 1. Experimental setup to generate zero mean, homogenous and isotropic turbulence along with an air-assist atomizer to generate polydispersed droplets.

The air turbulence generated in the rig is characterized by the two-dimensional Particle Image Velocimetry (PIV) technique. The 'box of turbulence' room is fully seeded with seeding particles generated from a fog generator. Typically, the size of the particles generated by the fog generator is less than 3 µm. The particles are illuminated by a double pulse Nd: YAG laser (Quantel, Evergreen: 145 mJ/pulse at 532 nm; 5 mm beam diameter). The laser is made into a sheet (height 5 cm and waist 1 mm) before viewing. It is synchronously operated with a charge coupled device (CCD) camera (PCO pixelfly: 14 bit) by using a National instruments card (NI cDAQ). The camera is operated in double shutter mode with a pulse separation time of 100 µs. The viewing area is 3.4 cm x 4.8 cm at the centre of the box with a spatial resolution of 34 µm/pixel. For each operating condition, approximately 1000 PIV images are taken.

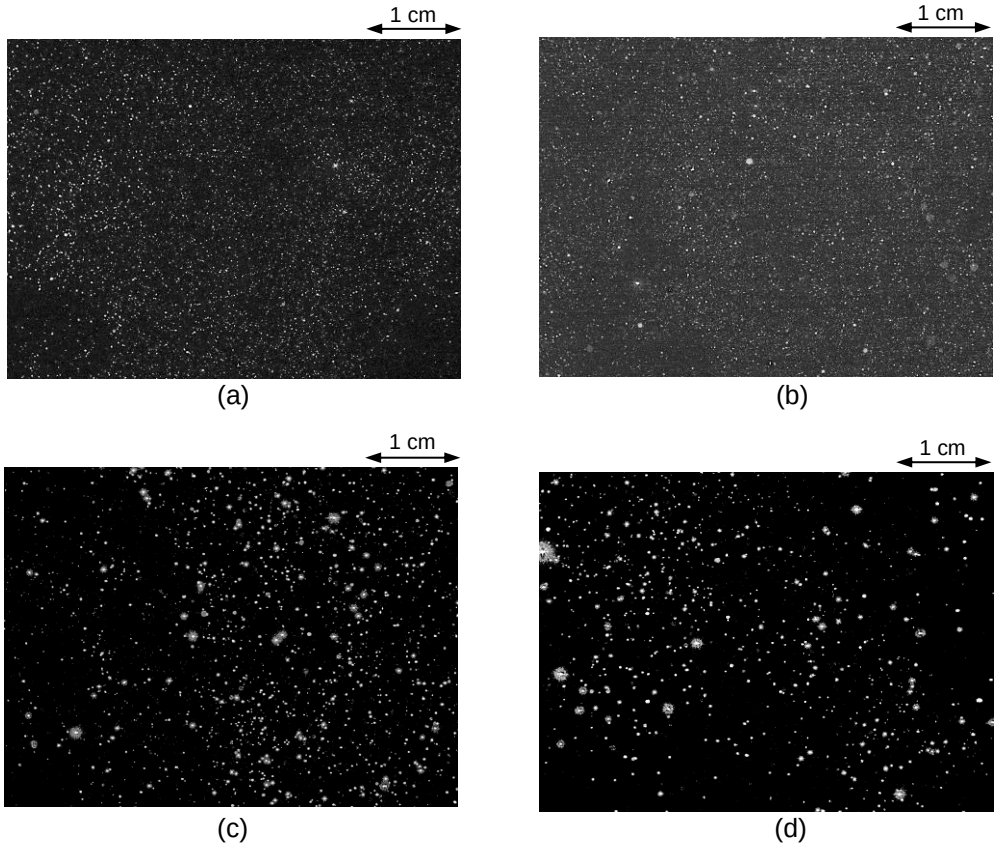

Figure 2. PIV images of droplets from the experiments a) acetone without HIT, b) acetone with HIT, c) water without HIT, and d) water with HIT

Polydisperse acetone droplets are generated using air assist internal type mixing atomizer (Spraying system Co. 1/4J series) mounted above the center of the box. Also, the spray loses its memory after a certain distance from the injector exit for this injector type. The injector has two opposite inlets for liquid and air. The inlet flow condition is maintained at 25 mLPM for liquid and 10 LPM for air. The atomizer is mounted at 90 cm above the center of the box such that the droplets has less momentum while entering the box of turbulence. Thus, the influence of droplets on air turbulence is avoided. Also, the local volume fraction (φ_v) at the given downstream location for the operating flow condition is less than 1 x 10^{-6}. So the droplets are one way coupled with the airflow, indicating that the HIT is not altered much by the droplets [7].The viewing area is maintained the same as that of PIV experiments. A total of 1000 image pairs are captured for each experiment. The droplet sizing is done using Interferometric Laser Imaging for Droplet Sizing (ILIDS) technique [8]. The PIV and ILIDS images are processed by using in-house image processing codes. The droplet clustering is studied with and without operating the box of turbulence for an evaporating acetone spray and

water spray. Typical PIV images from droplet experiments are shown in Fig 2. The acetone droplets without and with HIT are shown in Fig 2a and 2b, respectively. The water droplets without and with HIT are given in Fig 2c to 2d, respectively. From the figure, it can be seen that the number density of acetone droplets is more compared to the water case, either in the presence or absence of the HIT.

2.2. Image processing for droplet cluster characterization

In the present work, the PIV images of droplets are used to calculate Voronoi tessellations to identify individual droplet clusters. Each particle/droplet is associated with a cell in a Voronoi diagram. A Voronoi cell is defined as the ensemble of points closer to a particle than to any other [9]. For a given particle, its Voronoi area depends on the relative distance between other particles. If the particles are closely arranged at some location, the Voronoi areas are smaller, and if the particles are sparsely located, the Voronoi areas are larger. Thus, the Voronoi area directly represents local particle concentration in a flow field, and it is inversely proportional to the local concentration. So the calculation of the Voronoi area in the spray image can facilitate identifying the distribution of clusters of droplets. The steps for identifying the individual clusters in an instantaneous PIV image (Fig 3a) are explained below. The first step is to identify the position of the droplets in a PIV image. For this purpose, the PIV images are converted to binary images using a thresholding technique based on Otsu's method. The resulting image contains the droplet positions (Fig 3b). Each dot in the image represents the centroid of identified droplets from the PIV image. Voronoi cells are calculated for the identified centroids. The individual area of the Voronoi cells is calculated. The experimental area PDF is compared with a PDF of randomly distributed droplets to identify the cells that belong to clusters. In most cases, the two distributions meet at two points. The probability of the normalized cell areas should be higher than the RPP to classify them as either clusters or voids. The Voronoi cell areas smaller than the first intersection point are considered cluster cells, and those larger than the second intersection point are considered void cells. Then the individual clusters are identified by grouping the cells which share a common vertex. The identified clusters are shown using red colour in Fig 3c.

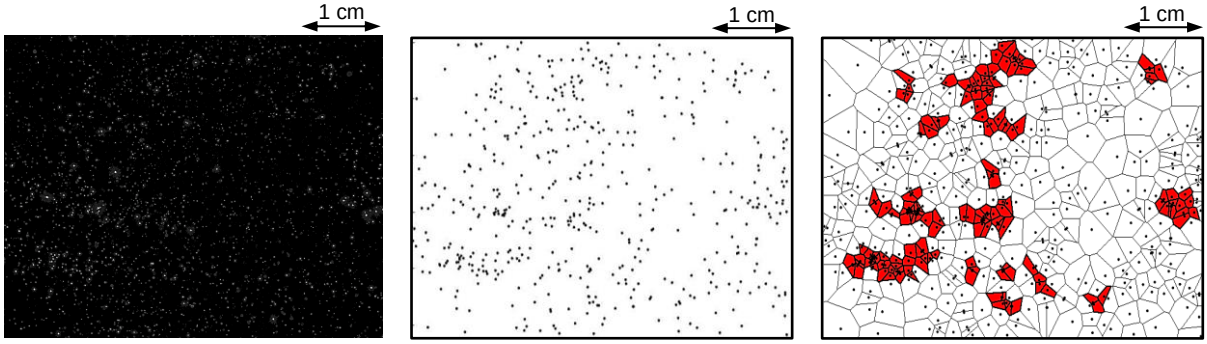

Figure 3. a) A raw PIV image of droplets from the experiment, b) Identified droplet centers using Otsu's technique, and c) Individual clusters have shown using red colour

3. Results and Discussion

3.1. Turbulence characterization in the box (without the spray)

The air turbulence created by the experimental rig is measured from the PIV images of the seeding particles (in the absence of spray injection). Only one turbulence condition is reported in this work, and droplet clustering is studied for that case. The instantaneous air velocity in the x- and y-directions (denoted by U_g and V_g, respectively) before introducing droplets is measured using a cross-correlation technique with an interrogation window size of 32x32

pixel^2 with 50% overlap and a search window size of 64x64 pixel^2. From the instantaneous air velocity, the mean component of velocity ($\bar{U}_g$ and $\bar{V}_g$) is calculated. The mean velocity contour plots (not shown here) indicates the turbulence with a mean flow of less than 0.1 m/s in both directions. Thus, the air turbulence created has statistically zero mean flow in the region of interest. The spatial mean of RMS of velocity fluctuations $U_{g,RMS}$ and $V_{g,RMS}$ is found to be 0.31 and 0.30, respectively. The spatial map of isotropy ($U_{g,RMS}/V_{g,RMS}$) contour plot is shown in Fig 4a. It indicates that the ratio of RMS fluctuations varies between 0.9 to 1.3, with a spatial average of 1.05. The longitudinal (R_{xx} and R_{yy}) and lateral (R_{xy} and R_{yx}) velocity correlation coefficients in the x- and y-directions are calculated and presented in Fig 4b. It can be seen that there is a good agreement between the longitudinal correlations. The same trend is observed for lateral velocity correlations as well. This further confirms the isotropic nature of the box of turbulence.

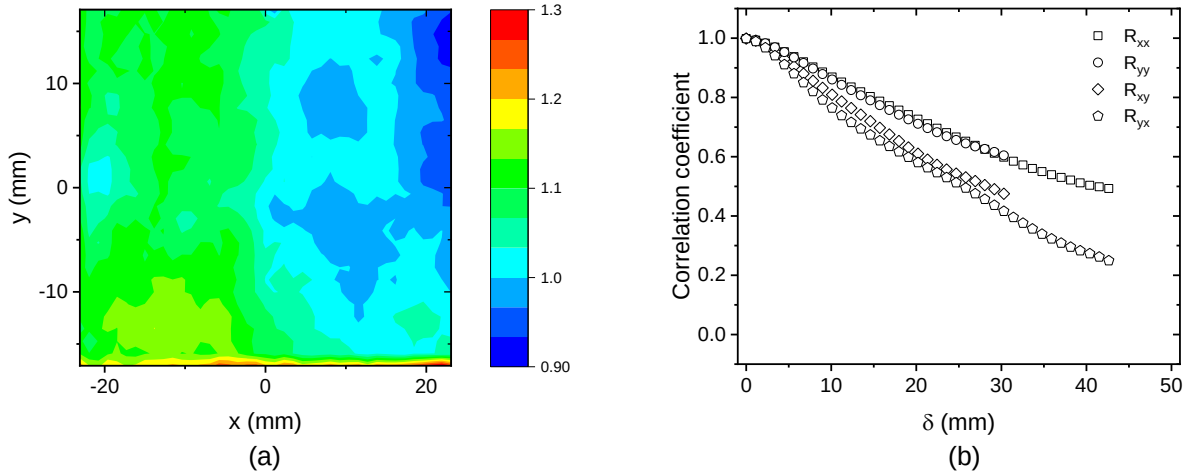

Figure 4. a) Contour plot of isotropy in the region of interest and b) two-point longitudinal and lateral velocity correlation coefficients

3.2. Droplet size and velocity (in the absence and presence of HIT)

The arithmetic mean diameter (AMD) and sauter mean diameter (SMD) of the droplet are calculated from the ILIDS data. AMD is used to calculate particle relaxation time, and the Stokes number is estimated using the large-eddy time scale (*St*) as well as the Kolmogorov time scale (St_η), and the values are shown in Table 1. A detailed description of Stokes number evaluation can be found elsewhere [8]. From table 1, both AMD and SMD are smaller for acetone droplets compared with water droplets. For acetone, in the absence of HIT, the *St* and St_η are 0.01 and 0.4, respectively. The St_η value is close to 'one' indicating the droplets respond well to the small-scale turbulence. In the presence of HIT, both the values of *St* and St_η increased to 0.02 and 0.7, respectively, and the response of droplets to similar size eddies slightly improved compared with the previous case. For water, in the absence of HIT, the *St* and St_η are 0.06 and 2.4, respectively. It is interesting to see both *St* and St_η are increased in the presence of HIT, but the St_η is moving away from 'one'. This indicates the response of droplets with large-scale turbulence is improved but with small-scale turbulence is decreased.

Table 1 – Drop size and Stokes number comparison for acetone and water droplets

Description	Acetone	Acetone (HIT)	Water	Water (HIT)
AMD (µm)	16.4	17.3	34.6	34.7
SMD (µm)	32.4	34.4	51.7	53.6
St based on *AMD*	0.01	0.02	0.06	0.08
St_η based on *AMD*	0.4	0.7	2.4	3.5

The average velocity of droplets and gas (in the absence of droplets) along the horizontal centerline are shown in Fig 6a and 6b for acetone and water, respectively. It can be observed that both the mean velocity ($\bar{U}_g$ and $\bar{V}_g$) for gas are close to zero. It is due to the turbulence generated having statistically zero mean flow. The variation of the mean velocity of air is insignificant along the x-direction due to the homogeneity of the created turbulence. Figure 6a shows the variation of mean velocity for acetone droplets. The mean y-velocity ($\bar{V}$) is high compared to x-velocity ($\bar{U}$). In the presence of HIT, there is a reduction in y-velocity but an improvement in x-velocity. This indicates the influence of turbulence on droplet velocity and brings both the mean velocity close to each other. The variation of mean velocity for water droplets is shown in Fig 6b, which also indicates similar results as that of acetone. It is interesting to see that even though the same external turbulence intensity is used for acetone and water, their velocity modulation is not the same.

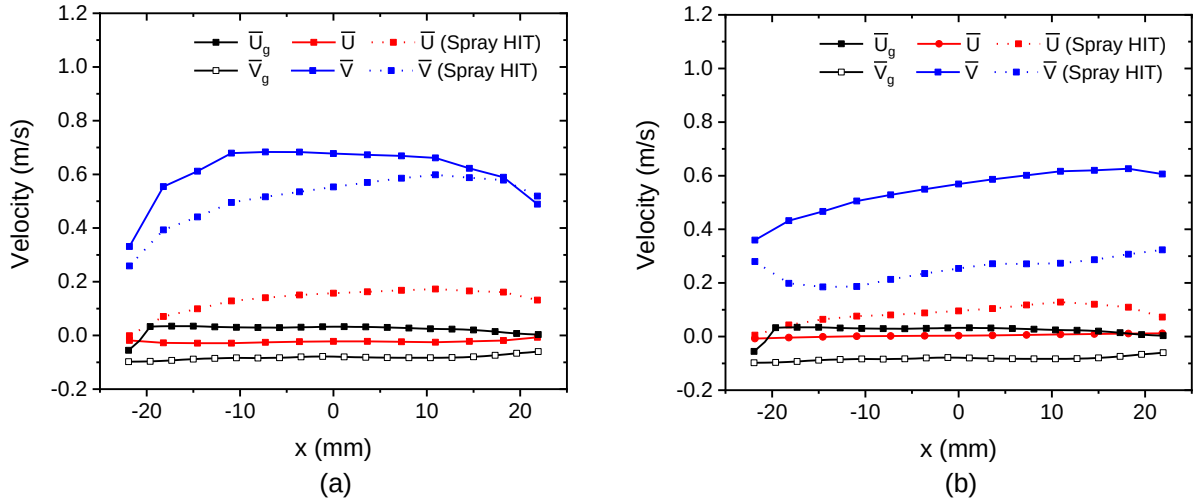

Figure 6. Ensemble averaged velocity along x-direction for a) acetone and b) water droplets

The RMS of velocity fluctuations for acetone and water is shown in Fig 7a and 7b, respectively. It can be seen that both the RMS fluctuations of the gas phase ($U_{g,RMS}$ and $V_{g,RMS}$) are close to 0.3 and invariant along the x-direction. For acetone, in the absence of HIT, the RMS of y-velocity fluctuations (V_{RMS}) are high and x-velocity fluctuations (U_{RMS}) are less compared with the RMS fluctuations of the gas phase. The same trend is maintained even in the presence of HIT. But for water, both U_{RMS} and V_{RMS} are less compared with the RMS fluctuations of the gas phase.

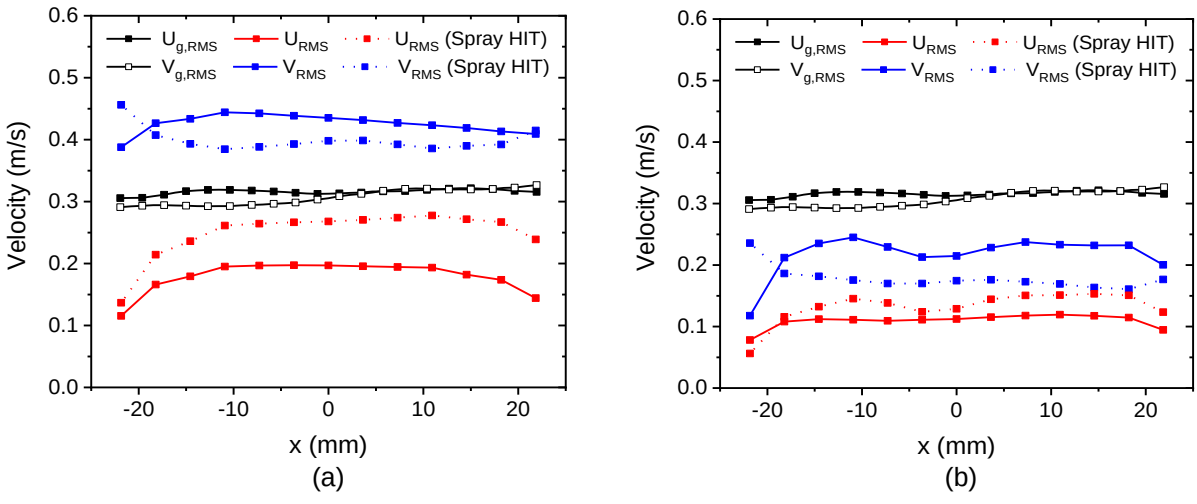

Figure 7. Ensemble averaged RMS of velocity fluctuations along x-direction for a) acetone and b) water droplets

3.3. Droplet cluster area distribution

Figure 8a and 8b show the cluster area PDFs for acetone and water droplets, respectively. Interestingly, for acetone the PDFs overlap except for the small-scale clusters for where the PDF is slightly higher in the presence of HIT. From Fig 8b, it can be observed that for water, in the presence of HIT, there is a considerable shift in the PDF. Thus, the probability of small clusters reduces, while that of large clusters is higher. As far as the behaviour of small clusters are considered, the above results can be explained on the basis of St_η. Notice that in Table 1, due to HIT, St_η apporaches 'one' for the acetone spray, which indicates stronger clustering. On the other hand, for the water spray St_η increases from 2.4 to 3.5 which suggest reduced tendency to cluster. However, for no much difference occurs for the Stokes number based on large scale, St either for the acetone or the water spray in the presence of HIT. In addition, St is not much different for acetone and water droplets as $St \ll 1$ for both cases. Yet, clustering is stronger for the water spray at larger scale. However, no difference is evident for the acetone spray. This suggests some role of rate of evaporation of droplets on clustering at large scale. Further investigations are currently being carried out in this direction.

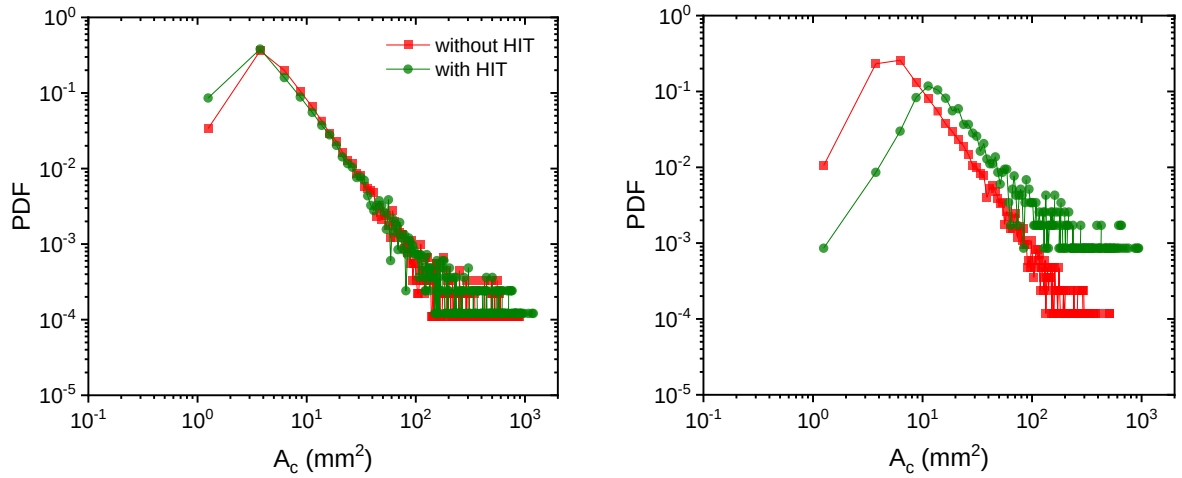

Figure 8. Droplet cluster area distribution with and without HIT for a) acetone and b) water sprays

3.4. Degree of droplet clustering

The degree of clustering is evaluated by comparing the standard deviation of normalized Voronoi areas (σ_v) with the standard deviation of RPP (σ_{RPP}) distribution. For the 2D area distribution σ_{RPP} is 0.53 [10]. The parameter σ_{rel} is calculated by the equation given below

$$\sigma_{rel} = \frac{\sigma_v - \sigma_{RPP}}{\sigma_{RPP}}$$

The positive value of σ_{rel} indicates a non-random distribution of Voronoi areas. Table 2 presents the degree of droplet clustering for acetone and water droplets. It can be seen that the degree of clustering is always positive, which indicates the droplets are always clustering even without the external air turbulence. It can be observed that the clustering of acetone droplets is enhanced in the presence of HIT. However, the difference in σ_{rel} is much smaller for the acetone spray in comparison to the water spray. In the case of water droplets, the degree of droplet clustering increased by approximately three folds. These results are in agreement with the cluster area PDF's presented earlier.

Table 2 – Degree of droplet clustering for acetone and water droplets with and without HIT

Degree of droplet clustering	Without HIT	With HIT
Acetone	1.58	2.10
Water	0.80	2.22

4. Conclusions

Experiments are conducted to study the clustering of evaporating droplets in homogeneous and isotropic turbulence with nearly zero mean flow. An air-assist atomizer is used to inject polydispersed acetone droplets into the center of the HIT region. Cluster characterization is done using Voronoi analysis on particle image velocimetry images of the droplets. Experiments are also conducted with water droplets. The key observations are summarized below.

1. For both, in the presence and absence of HIT, the mean velocity and RMS of velocity fluctuations are higher for acetone droplets in comparison to the water droplets.
2. The cluster area PDF almost overlaps for acetone droplets except for the small-scale clusters. The cluster area PDF in the presence of HIT shifts more to the right for water droplets. This is in agreement with the calculated magnitude of the degree of clustering.
3. In the presence of HIT, the difference in the evolution of small-scale clusters between the two sprays could be explained in terms of St_η.
4. The difference in the evolution of large scale clusters between the two sprays, in spite of having similar *St*, suggest some role of droplet evaporaton rate on the tendency of droplets for clustering.

References

[1] Balachandar, S., and Eaton, J. K., 2010, “Turbulent Dispersed Multiphase Flow,” Annu. Rev. Fluid Mech., **42**(1), pp. 111–133.
[2] Hwang, W., and Eaton, J. K., 2004, “Creating Homogeneous and Isotropic Turbulence without a Mean Flow,” Exp. Fluids, **36**, pp. 444–454.
[3] Birouk, M., Chauveau, C., Sarh, B., Quilgars, A., and Gökalp, I., 1996, “Turbulence Effects on the Vaporization of Monocomponent Single Droplets,” Combust. Sci. Technol., **113**–**114**(October 2014), pp. 413–428.
[4] Charalampous, G., and Hardalupas, Y., 2011, “Preferential Concentration of Water Droplets in a Volume of Homogeneous and Isotropic Turbulence,” (January), pp. 1–8.
[5] Marie, C. G. J., Chareyron, D., and Lance, M., 2010, “Characterization of a System Generating a Homogeneous Isotropic Turbulence Field by Free Synthetic Jets,” Exp. Fluids, pp. 809–822.
[6] Patel, U., and Sahu, S., 2019, “Effect of Air Turbulence and Fuel Composition on Bi-Component Droplet Evaporation,” Int. J. Heat Mass Transf., **141**, pp. 757–768.
[7] Lian, H., and Charalampous, G., 2013, “Preferential Concentration of Poly-Dispersed Droplets in Stationary Isotropic Turbulence,” Exp. Fluids.
[8] Manish, M., and Sahu, S., 2018, “Analysis of Droplet Clustering in Air-Assist Sprays Using Voronoi Tessellations,” Phys. Fluids, **30**(12).
[9] Monchaux, R., Bourgoin, M., and Cartellier, A., 2010, “Preferential Concentration of Heavy Particles: A Voronoï Analysis,” Phys. Fluids, **22**(10).
[10] Ferenc, J. S., and Néda, Z., 2007, “On the Size Distribution of Poisson Voronoi Cells,” Phys. A Stat. Mech. its Appl., **385**(2), pp. 518–526.